

Diffractive scattering at NLO in the dipole picture

Heikki Mäntysaari

University of Jyväskylä, Department of Physics
Centre of Excellence in Quark Matter
Finland



January 18, 2023 – XXIX The Cracow Epiphany Conference

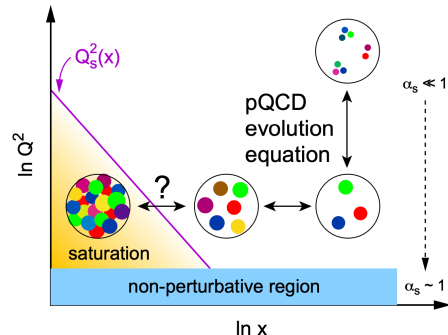
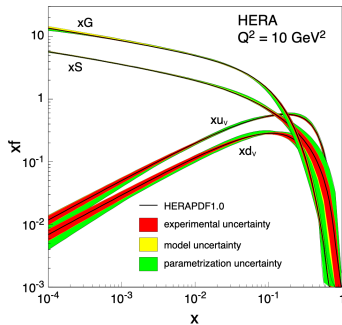


JYVÄSKYLÄN YLIOPISTO
UNIVERSITY OF JYVÄSKYLÄ



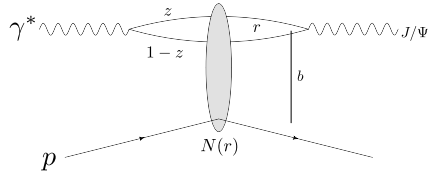
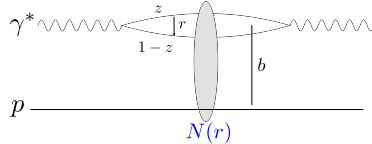
Non-linear dynamics at high energies

HERA total $\gamma^* + p$ cross section data: parton densities $\sim x^{-\lambda}$, eventually violates unitarity



Non-linear QCD effects at small x (e.g. $gg \rightarrow g$) should tame this growth
⇒ Saturated state of gluonic matter at small x and moderate Q^2 or M_X^2
Color Glass Condensate: effective theory of QCD in the high-density region

Probing high density gluonic matter in DIS: CGC and dipole picture



Inclusive cross section

Optical theorem:

$$\sigma^{\gamma^* p} \sim \Psi^* \otimes \Psi \otimes N$$

~ **dipole N** ~ “gluon structure”

Diffractive processes

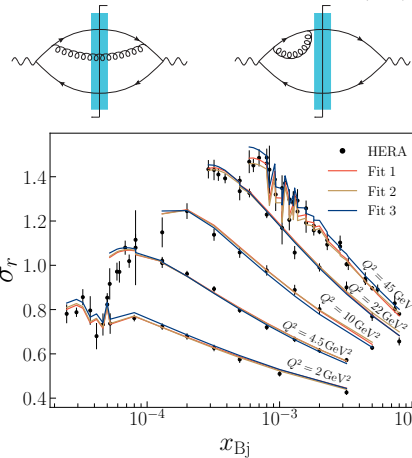
- Exclusive process:
 $\mathcal{A} \sim \int d^2 \mathbf{b} e^{-i\mathbf{b} \cdot \Delta} \Psi^* \otimes \Psi_V \otimes N$
- Diffractive structure function:
 $q\bar{q}$ mass in the final state M_X^2

- Dipole picture at high energy: $\gamma^* \rightarrow q\bar{q}$ fluctuation has a long lifetime \Rightarrow factorization
- **Dipole amplitude N** : eikonal propagation in the color field, resumming multiple scattering
Center-of-mass energy dependence perturbative: BK/JIMWLK

1. Inclusive baseline

Initializing small- x evolution from HERA structure function data

NLO accuracy: $|\gamma^*\rangle = |\gamma^*\rangle_0 + \Psi^{\gamma \rightarrow q\bar{q}}|q\bar{q}\rangle + \Psi^{\gamma \rightarrow q\bar{q}g}|q\bar{q}g\rangle + \dots$



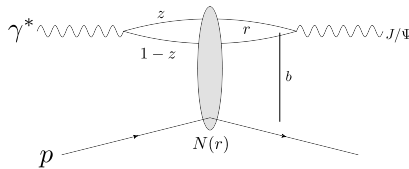
- $\sigma_r \sim |\Psi^{\gamma \rightarrow q\bar{q}}|^2 \otimes N + |\Psi^{\gamma \rightarrow q\bar{q}g}|^2 \otimes N_{q\bar{q}g} + \dots$
Large- N_c : $q\bar{q}g \approx q\bar{q} + q\bar{q} \Rightarrow N_{q\bar{q}g} \sim N \times N$
- **Photon wave functions** perturbative, known at NLO
[Beuf, Lappi, Paatelainen, 2103.14549, 2112.03158, 2204.02486](#)
- Perturbative energy (x) evolution for **N**: BK, need non-perturbative initial condition
- Fit initial dipole to HERA structure function data
- Excellent description of total and charm data possible (only at) NLO

[Hänninen, H.M, Paatelainen, Penttala, 2211.03504](#)

[Beuf, Hänninen, Lappi, H.M, 2007.01645](#)

2. Exclusive vector meson production at LO

Vector meson production



- $\gamma^* + p \rightarrow J/\psi + p$
- Need at least 2 gluons for exclusivity, very sensitive probe
- Momentum transfer measurable, conjugate to geometry
- New (non-perturbative) ingredient:
 - Meson wave function Ψ_V
 - Phenomenological models or NRQCD based expansion

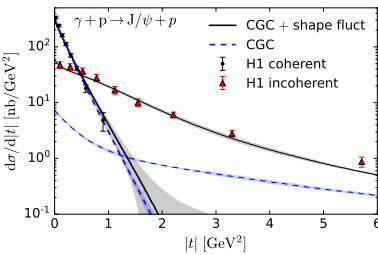
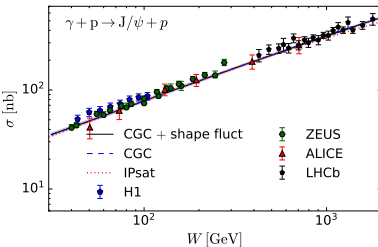
Lappi, H.M., Penttala, 2006.02830

Scattering amplitude in dipole picture

$$-i\mathcal{A}^{\gamma^* A \rightarrow VA} \sim \int d^2\mathbf{b} d^2\mathbf{r} \frac{dz}{4\pi} e^{-i\mathbf{b}\cdot\Delta} \Psi_{\gamma^*}^{q\bar{q}}(\mathbf{r}, z) \mathcal{N}(\mathbf{r}, \mathbf{b}, Y) \Psi_V^{q\bar{q}*}(\mathbf{r}, z)$$

*A particular advantage of the dipole picture:
simultaneous description of inclusive and diffractive observables
using the same degrees of freedom*

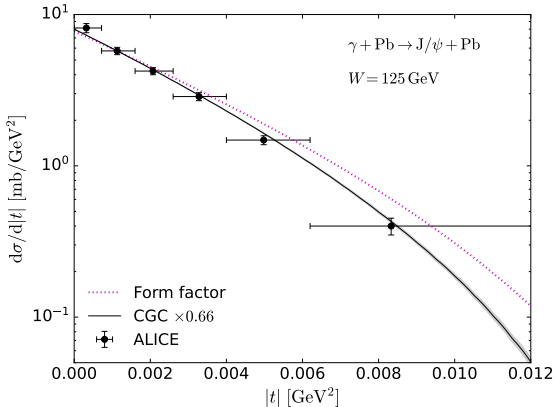
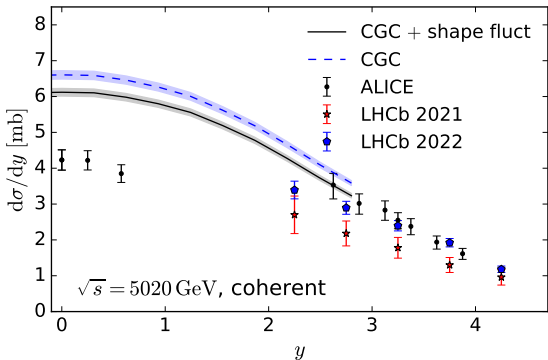
Successful LO phenomenology



H.M, Salazar, Schenke, 2207.03712

- Small- x vector meson production data described well
Kowalski, Motyka, Watt, [hep-ph/0606272](#)
- Coherent cross section up to $W \sim 2$ TeV well described, no clear deviations from W^δ powerlaw
- Geometry evolution requires some effective confinement prescription to regulate Coulomb tails
- Incoherent (proton dissociation) also well described (Sensitive to proton geometry fluctuations, see bakcup)

Successful LO phenomenology: nuclear targets in UPCs



- Ultra Peripheral Collisions at the LHC: coherent cross section at different $x_P \sim e^{\pm y}$
- Non-linear effects needed to describe the t spectrum!
- Even more nuclear suppression in $\gamma + A \rightarrow \text{J}/\psi$ data than predicted

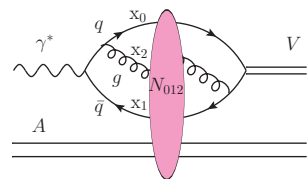
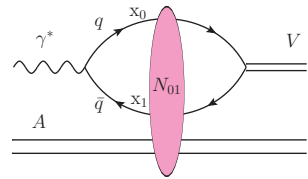
3. Vector meson production at NLO

Vector meson production at NLO

Invariant amplitude for exclusive vector meson production

$$\begin{aligned} -i\mathcal{A}_{t=0} &= 2 \int d^2\mathbf{x}_0 d^2\mathbf{x}_1 \int \frac{dz_0 dz_1}{(4\pi)} \delta(z_0 + z_1 - 1) \Psi_{\gamma^*}^{q\bar{q}} N_{01} \Psi_V^{q\bar{q}*} \\ &+ 2 \int d^2\mathbf{x}_0 d^2\mathbf{x}_1 d^2\mathbf{x}_2 \int \frac{dz_0 dz_1 dz_2}{(4\pi)^2} \delta(z_0 + z_1 + z_2 - 1) \Psi_{\gamma^*}^{q\bar{q}g} N_{012} \Psi_V^{q\bar{q}g*} \end{aligned}$$

- $|q\bar{q}g\rangle$ state also contributes, need meson wave function Ψ_V
 - for the $q\bar{q}g$ component ($\Psi_V^{q\bar{q}g}$) at tree level
 - for the $q\bar{q}$ component ($\Psi_V^{q\bar{q}}$) at one loop
 - Photon wave function Ψ_{γ^*} and dipole N as in inclusive DIS



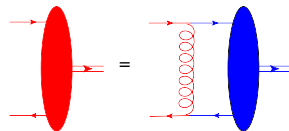
Nonrelativistic expansion for heavy quarkonium

Nonrelativistic expansion Escobedo, Lappi, 1911.01136

Meson wave function for the Fock state $|n\rangle$:

$$\Psi_V^n = \sum_{m,k} \underbrace{C_{n \leftarrow m}^k}_{\text{perturbative corrections}} \underbrace{\int_0^1 \frac{dz'}{4\pi} \left(\frac{1}{m_q} \nabla \right)^k \phi^m(\mathbf{r} = 0, z')}_{\text{nonperturbative constant}}$$

- ϕ^m = leading-order wave function for Fock state m
- α_s corrections included in perturbative $C_{n \leftarrow m}^k$ terms
- Relativistic corrections go as v^k in the index k

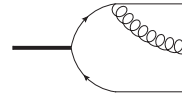
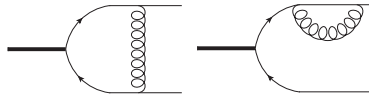


Escobedo, Lappi, 1911.01136

NLO calculation in the nonrelativistic limit

- Nonrelativistic limit: Leading-order wave function $\phi^{q\bar{q}}(\vec{k}) \sim (2\pi)^3 \delta^3(\vec{k})$
- Add perturbative corrections: $|V\rangle = \Psi_V^{q\bar{q}} |q\bar{q}\rangle + \Psi_V^{q\bar{q}g} |q\bar{q}g\rangle + \text{higher orders}$
- Only include the leading terms $\mathcal{O}(v^0)$ in heavy quark velocity:

$$\Psi_V^{q\bar{q}} = C_{q\bar{q} \leftarrow q\bar{q}}^0 \int_0^1 \frac{dz'}{4\pi} \phi^{q\bar{q}}(\mathbf{r} = 0, z') \quad \Psi_V^{q\bar{q}g} = C_{q\bar{q}g \leftarrow q\bar{q}}^0 \int_0^1 \frac{dz'}{4\pi} \phi^{q\bar{q}}(\mathbf{r} = 0, z')$$



- $C_{q\bar{q} \leftarrow q\bar{q}}^0, C_{q\bar{q}g \leftarrow q\bar{q}}^0$ at $\mathcal{O}(\alpha_s)$ calculated at [Escobedo, Lappi, 1911.01136](#)
- $\int_0^1 \frac{dz'}{4\pi} \phi^{q\bar{q}}(\mathbf{r} = 0, z')$ non-perturbative constant, related to decay width

Cancellation of divergences

- UV divergences between the $q\bar{q}$ and $q\bar{q}g$ parts of the calculation cancel
 - IR divergences cancel when we take into account:
 - Renormalization of the leading-order wave function $\phi^{q\bar{q}}(\vec{r} = 0)$
 - Can be related to the dimensionally regularized wave function [Escobedo, Lappi, 1911.01136](#)
$$\int \frac{dz'}{4\pi} \phi^{q\bar{q}} = \int \frac{dz'}{4\pi} \phi_{\text{DR}}^{q\bar{q}} \times \left[1 - \frac{\alpha_s C_F}{2\pi} \frac{1}{\alpha} \right], \alpha = \text{gluon IR cutoff}$$
 - The rapidity dependence of the dipole amplitude (BK)
- ⇒ The total production amplitude is finite and can be numerically evaluated

Also relativistic corrections included ⇒ NLO cross section at $\mathcal{O}(\alpha_s v^0, \alpha_s^0 v^2)$

- Longitudinal production: [H.M, Penttala, 2104.02349](#)
- Transverse production: [H.M, Penttala, 2204.14031](#)

Final expression (transverse production, $\mathcal{O}(\alpha_s v^0)$)

$$-i\mathcal{A}^T = \int \frac{dz'}{4\pi} \phi_{\text{DR}}^{q\bar{q}} \times \sqrt{\frac{N_c}{2}} \frac{ee_f m_q}{\pi} 2 \int d^2 \mathbf{x}_{01} \int d^2 \mathbf{b} \left\{ \mathcal{K}_{q\bar{q}}^{\text{LO}}(Y_0) + \frac{\alpha_s C_F}{2\pi} \mathcal{K}_{q\bar{q},\Psi}^{\text{NLO}}(Y_{\text{dip}}) + \frac{\alpha_s C_F}{2\pi} \int d^2 \mathbf{x}_{20} \int_{z_{\min}}^{1/2} dz_2 \mathcal{K}_{q\bar{q}g}(Y_{q\bar{q}g}) \right\}$$

where $\mathcal{K}_{q\bar{q}}^{\text{LO}}(Y_0) = K_0(\zeta) N_{01}(Y_0)$, $\zeta = |\mathbf{x}_{01}| \sqrt{\frac{1}{4} Q^2 + m_q^2}$,

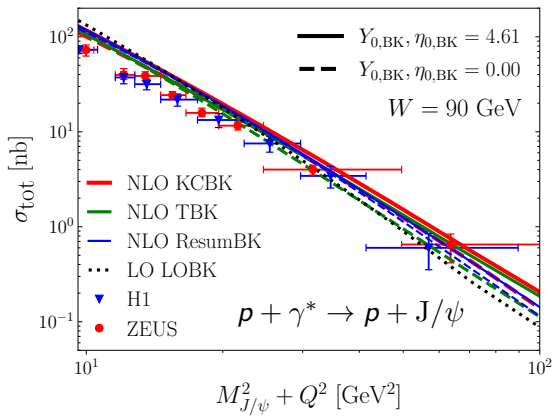
$$\mathcal{K}_{q\bar{q},\Psi}^{\text{NLO}} = \left[I_{\mathcal{VMS}}^T \left(\frac{1}{2}, \mathbf{x}_{01} \right) + \mathcal{K}^T + K_0(\zeta) \left(-\Omega_{\mathcal{V}}^T \left(\gamma; \frac{1}{2} \right) + L \left(\gamma; \frac{1}{2} \right) - \frac{\pi^2}{3} + \frac{5}{2} - 3 \ln \left(\frac{m_q |\mathbf{x}_{01}|}{2} \right) - 3\gamma_E \right) \right] N_{01}$$

and

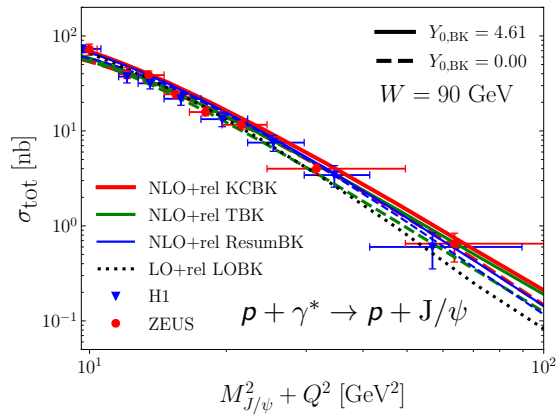
$$\begin{aligned} \mathcal{K}_{q\bar{q}g}(Y_{q\bar{q}g}) = & 32\pi m_q \left\{ K_1(2m_q z_2 |\mathbf{x}_{20}|) \frac{i \mathbf{x}_{20}^i}{|\mathbf{x}_{20}|} \left[-\mathcal{I}_{(j)}^i ((1-z_2)^2 + z_2^2) - z_2^2 (2z_2 - 1) \hat{\mathcal{I}}_{(j)}^i + \mathcal{I}_{(k)}^i \frac{1}{2z_2 + 1} + \hat{\mathcal{I}}_{(k)}^i \frac{z_2^2 (2z_2 - 1)^2}{(2z_2 + 1)^2} \right] N_{012} \right. \\ & + \frac{z_2}{m_q} K_0(2m_q z_2 |\mathbf{x}_{20}|) \left[\frac{-1 + 2z_2}{2} \mathcal{I}_{(j)}^{ii} + \frac{1 + 2z_2}{2} \mathcal{I}_{(k)}^{ii} - 2(1 - 2z_2) z_2 \mathcal{J}_{(l)} - 4m_q^2 z_2^2 \mathcal{I}_{(j)} \right] N_{012} \\ & \left. - ((1-z_2)^2 + z_2^2) \frac{1}{8\pi^2 m_q z_2 |\mathbf{x}_{20}|^2} K_0(\zeta) e^{-\mathbf{x}_{20}^2 / (\mathbf{x}_{10}^2 e^{\gamma_E})} N_{01} \right\}. \end{aligned}$$

NLO phenomenology

Nonrelativistic limit

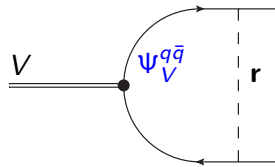


With v^2 relativistic corrections



- NLO corrections moderate, get a good description of HERA data
- Relativistic (v^2) corrections important at low Q^2

Light meson production at high Q^2

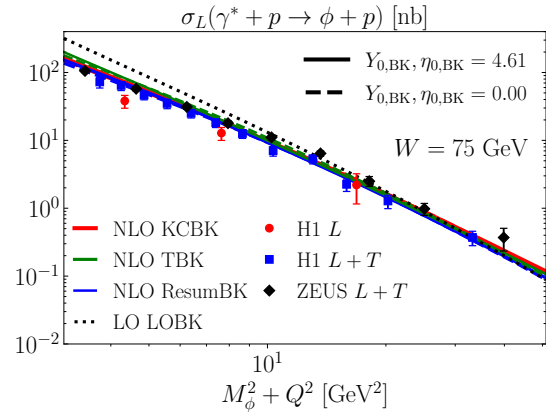
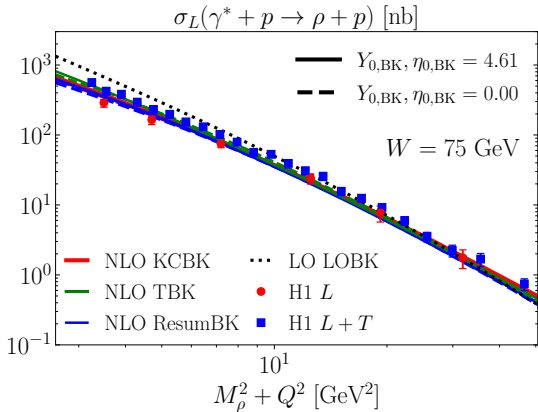


Now high Q^2 and light relativistic quarks

- High $Q^2 \Rightarrow$ only small dipole sizes r contribute,
 $\Psi_V^{q\bar{q}}(\mathbf{r}, z) \approx \Psi_V^{q\bar{q}}(0, z) \sim \phi(z)$
- $\phi(z)$: leading-twist distribution amplitude (DA)

- NLO corrections to meson wave function: LCPT calculation
- Scale dependence of the renormalized DA: ERBL equation \Rightarrow cancel divergences
- All dependence on the vector meson species included in the DA
- Expansion in Gegenbauer polynomials (but coefficients for ρ and ϕ not well known)
- Finite cross section for dominant longitudinal polarization: [H.M, Penttala, 2203.16911](#)

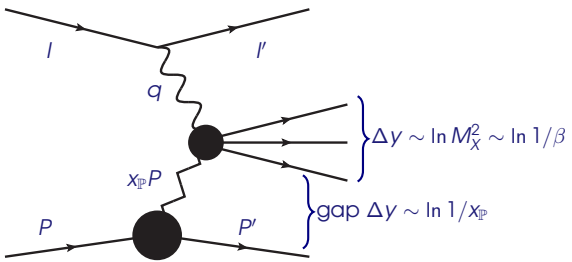
ρ and ϕ production – dependence on the photon virtuality Q^2



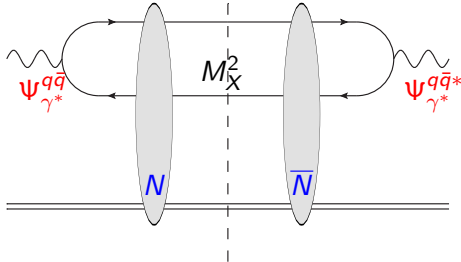
- Good description of HERA data, except ϕ at low Q^2
- NLO corrections improve the agreement with the data

H.M, Penttala, 2203.16911

4. Diffractive structure functions



Diffractive structure functions



Diffractive cross section as a function of M_X^2

- No need to model non-perturbative meson wave function
- Varying M_X^2 gives access to different photon Fock state components:
 $q\bar{q}g$ dominates at high M_X^2

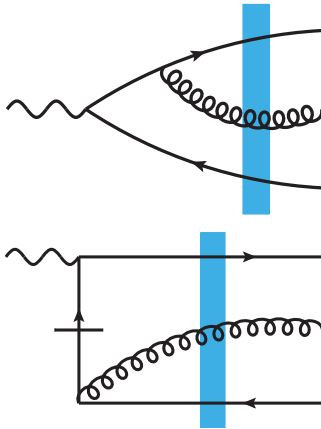
Inclusive diffraction cross section at LO ($q\bar{q}$ state)

$$\frac{d\sigma^D}{dM_X^2} = \frac{N_c}{4\pi} \int dz d^2\mathbf{r} d^2\bar{\mathbf{r}} d^2\mathbf{b} \mathcal{I}_{M_X}^{(2)} \textcolor{blue}{N\bar{N}} \textcolor{red}{\Psi_{\gamma^*}^{q\bar{q}}} \textcolor{red}{\Psi_{\gamma^*}^{q\bar{q}*}}$$

"Coordinates-to- M_X^2 transfer function" $\mathcal{I}_{M_X}^{(2)} = J_0 \left(M_X |\Delta\mathbf{r}| \sqrt{z(1-z)} \right)$

Diffractive $q\bar{q}g$ production

Example diagrams:



- NLO contribution where $|q\bar{q}g\rangle$ state interacts is finite (fixed M_X^2 requirement removes divergences)
- More complicated 3-particle transfer function $\mathcal{I}_{M_X}^{(3)}$ needed
- L and T cross sections in exact (eikonal) kinematics:

$$\begin{aligned}
 x_{\mathbb{P}} F_{L, q\bar{q}g}^{\text{D}(3) \text{ NLO}}(x, Q^2, \beta) = & 4 \frac{\alpha_s N_c C_F Q^4}{\beta} \sum_f e_f^2 \int_0^1 \frac{dz_0}{z_0} \int_0^1 \frac{dz_1}{z_1} \int_0^1 \frac{dz_2}{z_2} \delta(z_0 + z_1 + z_2 - 1) \\
 & \times \int_{x_0} \int_{x_1} \int_{x_2} \int_{\bar{x}_0} \int_{\bar{x}_1} \int_{\bar{x}_2} \mathcal{I}_{M_X}^{(3)} \delta^{(2)}(\mathbf{b} - \bar{\mathbf{b}}) 4 z_0 z_1 Q^2 K_0(Q X_{012}) K_0(Q X_{\bar{0}\bar{1}\bar{2}}) \\
 & \times \left\{ z_1^2 \left[(2z_0(z_0 + z_2) + z_2^2) \left(\frac{\mathbf{x}_{20}}{\mathbf{x}_{20}^2} \cdot \left(\frac{\mathbf{x}_{\bar{2}\bar{0}}}{\mathbf{x}_{\bar{2}\bar{0}}^2} - \frac{1}{2} \frac{\mathbf{x}_{\bar{2}\bar{1}}}{\mathbf{x}_{\bar{2}\bar{1}}^2} \right) - \frac{1}{2} \frac{\mathbf{x}_{\bar{2}\bar{0}} \cdot \mathbf{x}_{21}}{\mathbf{x}_{\bar{2}\bar{0}}^2 \mathbf{x}_{21}^2} \right) + \frac{z_2^2}{2} \left(\frac{\mathbf{x}_{\bar{2}\bar{0}} \cdot \mathbf{x}_{21}}{\mathbf{x}_{\bar{2}\bar{0}}^2 \mathbf{x}_{21}^2} + \frac{\mathbf{x}_{20} \cdot \mathbf{x}_{\bar{2}\bar{1}}}{\mathbf{x}_{20}^2 \mathbf{x}_{\bar{2}\bar{1}}^2} \right) \right] \right. \\
 & + z_0^2 \left[(2z_1(z_1 + z_2) + z_2^2) \left(\frac{\mathbf{x}_{21}}{\mathbf{x}_{21}^2} \cdot \left(\frac{\mathbf{x}_{\bar{2}\bar{1}}}{\mathbf{x}_{\bar{2}\bar{1}}^2} - \frac{1}{2} \frac{\mathbf{x}_{\bar{2}\bar{0}}}{\mathbf{x}_{\bar{2}\bar{0}}^2} \right) - \frac{1}{2} \frac{\mathbf{x}_{20} \cdot \mathbf{x}_{\bar{2}\bar{1}}}{\mathbf{x}_{20}^2 \mathbf{x}_{\bar{2}\bar{1}}^2} \right) + \frac{z_2^2}{2} \left(\frac{\mathbf{x}_{\bar{2}\bar{1}} \cdot \mathbf{x}_{21}}{\mathbf{x}_{\bar{2}\bar{1}}^2 \mathbf{x}_{21}^2} + \frac{\mathbf{x}_{20} \cdot \mathbf{x}_{\bar{2}\bar{1}}}{\mathbf{x}_{20}^2 \mathbf{x}_{\bar{2}\bar{1}}^2} \right) \right] \Big] \\
 & \times \left[1 - S_{\bar{0}\bar{1}\bar{2}}^\dagger \right] \left[1 - S_{012} \right], \\
 \mathcal{I}_{M_X}^{(3)} = & 2 \frac{z_0 z_1 z_2}{(4\pi)^2} \frac{M_X}{Y_{012}} J_1(M_X Y_{012}), \quad Y_{012}^2 = z_0 z_1 (\mathbf{x}_{\bar{0}\bar{0}} - \mathbf{x}_{\bar{1}\bar{1}})^2 + z_1 z_2 (\mathbf{x}_{\bar{2}\bar{2}} - \mathbf{x}_{\bar{1}\bar{1}})^2 + z_0 z_2 (\mathbf{x}_{\bar{2}\bar{2}} - \mathbf{x}_{\bar{0}\bar{0}})^2.
 \end{aligned}$$

Beuf, Hänninen, Lappi, Mulian, H.M,

2206.13161

Reproduce known high- Q^2 limit

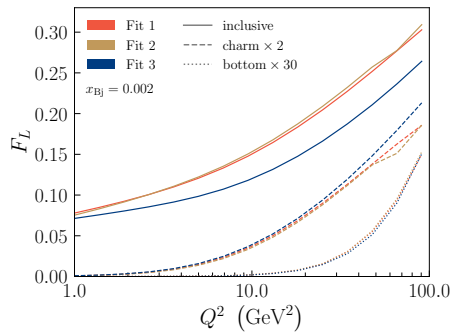
Wüsthoff, hep-ph/9702201, Golec-Biernat, Wüsthoff, hep-ph/9903358

Conclusions

Diffractive scattering processes in the dipole picture

- Successful phenomenology at LO
- CGC calculations are entering the precision era
 - Total and charm production cross section at NLO
 - Heavy quarkonium production at NLO in non-relativistic limit + 1st relativistic correction
 - Light meson production at NLO in the high- Q^2 limit
 - Progress towards diffractive structure functions at NLO:
 $q\bar{q}g$ production dominating at high- Q^2 available, loops in progress [Lappi, Paatelainen, Penttala, HM](#)
- First phenomenological applications at NLO available, compatible with HERA data

Complementary constraints from the EIC



- A few different NLO fits with equally good description of HERA data

[Beuf, Hänninen, Lappi, H.M, 2007.01645](#)

[Hänninen, H.M, Paatelainen, Penttala, 2211.03504](#)

- Predictions for F_L in the EIC kinematics still differ:
⇒ Complementary constraints from the EIC data
- Reason: F_L is sensitive to different dipole sizes
- These fits are necessary input to all NLO calculations

Exclusive processes: beyond average structure

Exclusive processes: no net color transfer, rapidity gap around the produced particle

Coherent diffraction:

- Target remains in the same quantum state, e.g.
 $\gamma + p \rightarrow J/\Psi + p$
- Probes average interaction

$$\frac{d\sigma^{\gamma^* A \rightarrow VA}}{dt} \sim |\langle \mathcal{A}^{\gamma^* A \rightarrow VA} \rangle_{\Omega}|^2$$

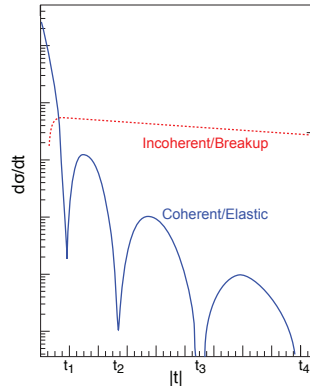
$\langle \rangle_{\Omega}$: average over target configurations Ω

Incoherent diffraction, the remaining events:

- E.g. $\gamma + p \rightarrow J/\Psi + p^*$ (+ dissociation $p^* \rightarrow X$).
- Total diffractive – coherent

$$\sigma_{\text{incoherent}} \sim \langle |\mathcal{A}|^2 \rangle_{\Omega} - |\langle \mathcal{A} \rangle_{\Omega}|^2$$

- Variance: sensitive to fluctuations



Good, Walker, PRD 120, 1960

Miettinen, Pumplin, PRD 18, 1978

Kovchegov, McLerran, PRD 60, 1999

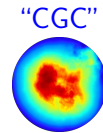
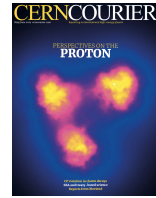
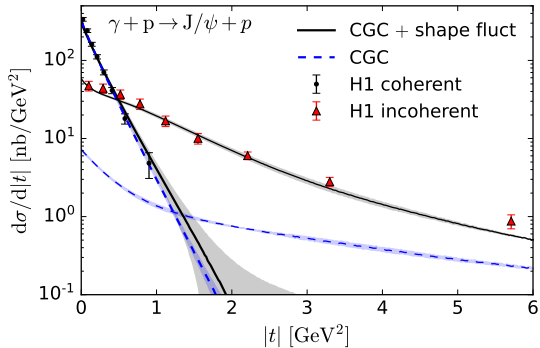
Kovner, Wiedemann, PRD 64, 2001

Caldwell, Kowalski, PRC 81, 2010

H.M., Rept. Prog. Phys. 83, 2020

Successful LO phenomenology: proton shape fluctuations at $x_P \approx 0.001$

Study simultaneously coherent (\sim average interaction) and incoherent (Δ variance)
CGC + shape fluct



- Parametrize e-b-e fluctuating geometry, fit parameters to data

Original: H.M., B. Schenke, 1607.01711 (PRL), recent: 2202.01998 (HM, Schenke, Shen, Zhao), similar setup e.g.: Bendova, Cepila, Contreras; Cepila, Contreras, Krelina, Takaki; Traini, Blaizot; Kumar, Toll